Fig 3. Effects of leuprorelin on mutant androgen receptor (AR) accumulation in scrotal skin, serum testosterone, and creatine kinase (CK). (A) Scrotal skin shows intense and frequent staining for anti-polyglutamine antibody in the nucleus before therapy. (B) Twelve weeks after therapy, both intensity and frequency of nuclear staining markedly decreased. Bar = $30\mu m$ (C) Quantitative analysis of immunohistochemistry demonstrated a significant decrease in the number of positively stained nuclei. (D) Serum testosterone and CK decreased significantly in 6 months. Frequency of staining was calculated from counts of more than 500 nuclei in randomly selected areas and was expressed as mean ± standard deviation for 5 patients. **$p < 0.01$; ***$p < 0.0001$.

Although our results were obtained from a small sample, nuclear accumulation of mutant AR in the scrotal skin appears to be a potent pathogenic biomarker of SBMA. A correlation between decline in validated clinical scales and nuclear mutant AR accumulations must be demonstrated in a longitudinal study to verify this histopathological feature as a biomarker for clinical severity. Similarly, validation of the scrotal skin biopsy findings as a surrogate end point in clinical trials will require a longitudinal study verifying that suppression of nuclear staining correlates with improvement on a validated clinical scale and the true clinical outcome events such as the need for a wheelchair, the presence of aspiration pneumonia, or death.

Banno et al: Scrotal Skin AR as SBMA Marker   525

References

1. Kennedy WR, Alter M, Sung JH. Progressive proximal spinal and bulbar muscular atrophy of late onset: a sex-linked recessive trait. Neurology 1968;18:671–680.
2. Sperfeld AD, Karitzky J, Brummer D, et al. X-linked bulbospinal neuropathy: Kennedy disease. Arch Neurol 2002;59: 1921–1926.
3. Sobue G, Hashizume Y, Mukai E, et al. X-linked recessive bulbospinal neuronopathy: a clinicopathological study. Brain 1989; 112:209–232.
4. Katsuno M, Adachi H, Tanaka F, et al. Spinal and bulbar muscular atrophy (SBMA): ligand-dependent pathogenesis and therapeutic perspective. J Mol Med 2004;82:298–307.
5. Sobue G, Adachi H, Katsuno M. Spinal and bulbar muscular atrophy (SBMA). In: Dickinson D, ed. Neurodegeneration: the molecular pathology of dementia and movement disorders. Basel: INS Neuropathology, 2003:275–279.
6. La Spada AR, Wilson EM, Lubahn DB, et al. Androgen receptor gene mutations in X-linked spinal and bulbar muscular atrophy. Nature 1991;352:77–79.
7. Tanaka F, Doyu M, Ito Y, et al. Founder effect in spinal and bulbar muscular atrophy (SBMA). Hum Mol Genet 1996;5: 1253–1257.
8. Doyu M, Sobue G, Mukai E, et al. Severity of X-linked recessive bulbospinal neuronopathy correlates with size of the tandem CAG repeat in androgen receptor gene. Ann Neurol 1992; 32:707–710.
9. Shimada N, Sobue G, Doyu M, et al. X-linked recessive bulbospinal neuronopathy: clinical phenotypes and CAG repeat size in androgen receptor gene. Muscle Nerve 1995;18: 1378–1384.
10. Zoghbi HY, Orr HT. Glutamine repeats and neurodegeneration. Annu Rev Neurosci 2000;23:217–247.
11. Li M, Miwa S, Kobayashi Y, et al. Nuclear inclusions of the androgen receptor protein in spinal and bulbar muscular atrophy. Ann Neurol 1998;44:249–254.
12. Li M, Nakagomi Y, Kobayashi Y, et al. Nonneural nuclear inclusions of androgen receptor protein in spinal and bulbar muscular atrophy. Am J Pathol 1998;153:695–701.
13. Arrasate M, Mitra S, Schweitzer ES, et al. Inclusion body formation reduces levels of mutant huntingtin and the risk of neuronal death. Nature 2004;431:805–810.
14. Katsuno M, Adachi H, Kume A, et al. Testosterone reduction prevents phenotypic expression in a transgenic mouse model of spinal and bulbar muscular atrophy. Neuron 2002;35: 843–854.
15. Katsuno M, Adachi H, Doyu M, et al. Leuprorelin rescues polyglutamine-dependent phenotypes in a transgenic mouse model of spinal and bulbar muscular atrophy. Nat Med 2003; 9:768–773.
16. Adachi H, Katsuno M, Minamiyama M, et al. Widespread nuclear and cytoplasmic accumulation of mutant androgen receptor in SBMA patients. Brain 2005;128:659–670.
17. Sobue G, Doyu M, Kachi T, et al. Subclinical phenotypic expressions in heterozygous females of X-linked recessive bulbospinal neuronopathy. J Neurol Sci 1993;117:74–78.
18. Schmidt BJ, Greenberg CR, Allingham-Hawkins DJ, Spriggs EL. Expression of X-linked bulbospinal muscular atrophy (Kennedy disease) in two homozygous women. Neurology 2002;59:770–772.
19. Takeyama K, Ito S, Yamamoto A, et al. Androgen-dependent neurodegeneration by polyglutamine-expanded human androgen receptor in Drosophila. Neuron 2002;35:855–864.
20. Chevalier-Larsen ES, O'Brien CJ, Wang H, et al. Castration restores function and neurofilament alterations of aged symptomatic males in a transgenic mouse model of spinal and bulbar muscular atrophy. J Neurosci 2004;24:4778–4786.
21. Shimohata T, Kimura T, Nishizawa M, et al. Five year follow up of a patient with spinal and bulbar muscular atrophy treated with leuprorelin. J Neurol Neurosurg Psychiatry 2004;75: 1206–1207.
22. Norris FH Jr, Calanchini PR, Fallat RJ, et al. The administration of guanidine in amyotrophic lateral sclerosis. Neurology 1974;24:721–728.
23. Trottier Y, Lutz Y, Stevanin G, et al. Polyglutamine expansion as a pathological epitope in Huntington's disease and four dominant cerebellar ataxias. Nature 1995;378:403–406.
24. Terao S, Sobue G, Hashizume Y, et al. Age-related changes in human spinal ventral horn cells with special reference to the loss of small neurons in the intermediate zone: a quantitative analysis. Acta Neuropathol (Berl) 1996;92:109–114.
25. DiFiglia M, Sapp E, Chase KO, et al. Aggregation of huntingtin in neuronal intranuclear inclusions and dystrophic neurites in brain. Science 1997;277:1990–1993.
26. Hayashi Y, Kakita A, Yamada M, et al. Hereditary dentatorubral-pallidoluysian atrophy: ubiquitinated filamentous inclusions in the cerebellar dentate nucleus neurons. Acta Neuropathol (Berl) 1998;95:479–482.
27. Paulson HL, Perez MK, Trottier Y, et al. Intranuclear inclusions of expanded polyglutamine protein in spinocerebellar ataxia type 3. Neuron 1997;19:333–344.
28. Biomarkers Definitions Working Group. Biomarkers and surrogate endpoints: preferred definitions and conceptual framework. Clin Pharmacol Ther 2001;69:89–95.
29. Fleming TR, DeMets DL. Surrogate end points in clinical trials: are we being misled? Ann Intern Med 1996;125: 605–613.
30. Temple R. Are surrogate markers adequate to assess cardiovascular disease drugs? JAMA 1999;282:790–795.

Disease Progression of Human SOD1 (G93A) Transgenic ALS Model Rats

Arifumi Matsumoto,[1,3,6] Yohei Okada,[1,4,6] Masanori Nakamichi,[5] Masaya Nakamura,[2] Yoshiaki Toyama,[2] Gen Sobue,[4] Makiko Nagai,[3] Masashi Aoki,[3] Yasuto Itoyama,[3] and Hideyuki Okano[1,6]*

[1]Department of Physiology, Keio University School of Medicine, Tokyo, Japan
[2]Department of Orthopaedic Surgery, Keio University School of Medicine, Tokyo, Japan
[3]Department of Neurology, Tohoku University Graduate School of Medicine, Sendai, Japan
[4]Department of Neurology, Nagoya University Graduate School of Medicine, Nagoya, Japan
[5]Takeda Chemical Industries, Ltd., Osaka, Japan
[6]Core Research for Evolutional Science and Technology (CREST), Japan Science and Technology Agency (JST), Saitama, Japan

The recent development of a rat model of amyotrophic lateral sclerosis (ALS) in which the rats harbor a mutated human SOD1 (G93A) gene has greatly expanded the range of potential experiments, because the rats' large size permits biochemical analyses and therapeutic trials, such as the intrathecal injection of new drugs and stem cell transplantation. The precise nature of this disease model remains unclear. We described three disease phenotypes: the forelimb-, hindlimb-, and general-types. We also established a simple, non-invasive, and objective evaluation system using the body weight, inclined plane test, cage activity, automated motion analysis system (SCANET), and righting reflex. Moreover, we created a novel scale, the Motor score, which can be used with any phenotype and does not require special apparatuses. With these methods, we uniformly and quantitatively assessed the onset, progression, and disease duration, and clearly presented the variable clinical course of this model; disease progression after the onset was more aggressive in the forelimb-type than in the hindlimb-type. More importantly, the disease stages defined by our evaluation system correlated well with the loss of spinal motor neurons. In particular, the onset of muscle weakness coincided with the loss of approximately 50% of spinal motor neurons. This study should provide a valuable tool for future experiments to test potential ALS therapies.   V 2005 Wiley-Liss, Inc.

Key words: amyotrophic lateral sclerosis; evaluation system; behavioral analyses; phenotype; variability

Amyotrophic lateral sclerosis (ALS) is a fatal neurodegenerative disorder that mainly affects the upper and lower motor neurons (de Belleroche et al., 1995). It is characterized by progressive muscle weakness, amyotrophy, and death from respiratory paralysis, usually within 3–5 years of onset (Brown 1995). Although most cases of ALS are sporadic (SALS), approximately 10% are familial (FALS) (Mulder et al., 1986). Moreover, 20–25% of FALS cases are due to mutations in the gene encoding copper-zinc superoxide dismutase (SOD1) (Deng et al., 1993; Rosen et al., 1993). More than 100 different mutations in the SOD1 gene have been identified in FALS so far.

Until recently, animal models of FALS have been various transgenic mice that express a mutant human SOD1 (hSOD1) gene. Of these, a transgenic mouse carrying the G93A (Gly-93 → Ala) mutant hSOD1 gene was the first described (Gurney et al., 1994) and is used all over the world because this model closely recapitulates the clinical and histopathological features of the human disease. To evaluate the therapeutic effects of potential ALS treatments in this animal, many motor-related behavioral tasks are used (Chiu et al., 1995; Barneoud et al., 1997; Garbuzova-Davis et al., 2002; Sun et al., 2002; Wang et al., 2002; Inoue et al., 2003; Kaspar et al., 2003; Weydt et al., 2003; Azzouz et al., 2004). However, transgenic mice have innate limitations for some types of experiments because of their small size.

Recently, transgenic rat models of ALS, which harbor the hSOD1 gene containing the H46R (His-46 → Arg) or G93A mutation were generated (Nagai et al., 2001). The larger size of these rat models makes certain experiments easier, such as biochemical analyses that require large amounts of sample, intrathecal administration

of drugs, and, especially, therapeutic trials, including the transplantation of neural stem cells into the spinal cord. The hSOD1 (G93A) transgenic rats typically present weakness in one hindlimb first. Later, weakness progresses to the other hindlimb and to the forelimbs. Finally, the rats usually become unable to eat or drink, and eventually die. Only subjective and ambiguous analyses were made with regard to the clinical progression of this ALS animal model and objective criteria for evaluating the efficacy of these new treatments have not been determined. For these reasons, we assessed the disease progression quantitatively using five different measures (body weight, inclined plane test, cage activity, SCA-NET, and righting reflex) and established an easy, non-invasive, and objective evaluation system that is sensitive to small but important abnormalities in the hSOD1 (G93A) transgenic rats. In addition, we created a novel scale, the Motor score, to assess disease progression in the transgenic rats without using special apparatuses. We also examined the validity of these measures as assessment tools for the pathology by investigating the number of spinal motor neurons remaining at the disease stages defined by each measure.

MATERIALS AND METHODS

Transgenic Rats

All animal experiments were conducted according to the Guidelines for the Care and Use of Laboratory Animals of Keio University School of Medicine. We used hSOD1 (G93A) transgenic male rats (Nagai et al., 2001) from our colony and their age- and gender-matched wild-type littermates as controls. Rats were housed in a specific pathogen-free animal facility at a room temperature of 23 6 18C under a 12-hr light-dark cycle (light on at 08:00). Food (solid feed CE-2, 30kGy; CLEA Japan, Inc.) and water were available ad lib. Transgenic rats were bred and maintained as hemizygotes by mating transgenic males with wild-type females. Transgenic progeny were identified by detecting the exogenous hSOD1 transgene, by amplification of pup tail DNA extracted at 20 days of age by polymerase chain reaction (PCR). The primers and cycling conditions were described previously (Nagai et al., 2001).

Exploration of Assessment Tools to Measure Disease Progression in the hSOD1 (G93A) Transgenic Rats

We evaluated the usefulness of four different measures to assess disease progression in the transgenic rats. All tests were carried out between 12:00–16:00 and in a double-blind fashion.

Body weight. Animals (n = 9 for each genotype) were weighed weekly after 30 days of age with an electronic scale. To avoid overlooking the beginning of weight loss, the animals were weighed every second or third day after 90 days of age, the age at which motor neurons are reported to be lost in the lumbar spinal cord (Nagai et al., 2001).

Inclined plane. This test was initially established mainly to assess the total strength of the forelimbs and hindlimbs in a model of spinal cord injury (Rivlin and Tator, 1977). Briefly, rats were placed laterally against the long axis of the inclined plane, and the maximum angle at which they

could maintain their position on the plane for 5 sec was measured. To assess the strength of both sides of limbs equally, animals were placed on the inclined plane with the right side of the body to the downhill side of the incline, and then with the left side of the body facing downhill. For each rat, the test was carried out three times for each side, and the mean value of the angles obtained for the right side was compared to that obtained for the left. The lower mean value was recorded as the angle for that rat. Animals (n = 9 for each genotype) were tested weekly after 70 days of age and every second to third day after 100 days of age.

Cage activity. Animals (n = 8 for each genotype) were housed individually and monitored every day for all 24 hr (except for the days the cages were changed) after they were 70 days old. Spontaneous locomotor activity in the home cage (345 3 403 3 177 mm) was recorded by an activity-monitoring system (NS-AS01; Neuroscience, Inc., Tokyo, Japan) as described previously (Ohki-Hamazaki et al., 1999). The sensor detects the movement of animals using the released infrared radiation associated with their body temperature. The data were analyzed by the DAS-008 software (Neuroscience, Inc., Tokyo, Japan). To eliminate data variability owing to differences in the baseline movement of each rat, the baseline value was calculated as the mean of movement from 70–90 days of age, during which all rats were considered to move normally. We analyzed the data at each time point as the percentage of the baseline value in defining disease onset with this test.

SCANET. For short-term activity, 10 min of spontaneous activity was measured with the automated motion analysis system SCANET MV-10 (Toyo Sangyo Co., Ltd., Toyama, Japan) (Mikami et al., 2002). Animals (n = 4 for each genotype) were tested weekly after 30 days of age and every second or third day after 100 days of age. Each rat was individually placed in the SCANET cage for 10 min. Three parameters were measured: small horizontal movements of 12 mm or more (Move 1; M1), large horizontal movements of 60 mm or more (Move 2; M2), and the frequency of vertical movements caused by rearing (RG). To distinguish RG movements from incomplete standing actions, the upper sensor frame was adjusted to 13 cm above the lower sensor frame.

Righting reflex. All affected animals were tested for the ability to right themselves within 30 sec of being turned on either side (righting reflex) (Gale et al., 1985). Failure was seen when animals reached the end-stage of disease (Howland et al., 2002), and was regarded as a generalized loss of motor activity. We used this time point, which we call "end-stage," as "death" rather than the actual death of the animal, to exclude the influence of poor food intake and respiratory muscle paralysis on the survival period. All end-stage animals were sacrificed after being deeply anesthetized.

All statistical analyses were carried out with the two-tailed unpaired Student's t-test. A P-value of <0.05 was considered statistically significant.

Motor Score

To establish our own scoring system for motor function, which could be uniformly applicable to any disease phenotype of this rat model, we examined the common clinical findings
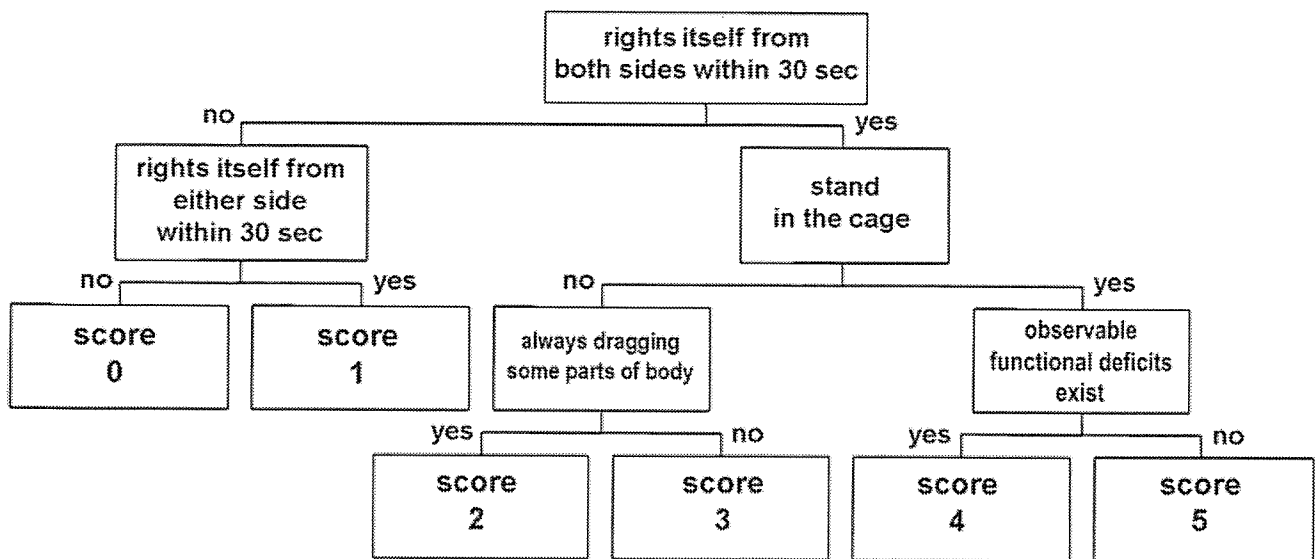
Fig. 1. Chart of Motor score assessment. The degree of motor dysfunction can be assessed by the Motor score as shown in this chart. This scoring system is meant to be used after disease onset, which can be prospectively diagnosed by the inclined plane test (muscle weakness onset). A score of 4 means the same condition as seen for subjective onset (SO). Rats with a score of 5 seem almost as normal as wild-type rats. The detailed testing procedure for the Motor score is described in the text.

of the transgenic rats in detail and assessed their motor functions (n = 20). We focused on the following tests: the righting reflex, the ability to stand in the cage, the extent of dragging their bodies when moving, and the existence of observable functional deficits. We evaluated these items sequentially along with the disease progression and classified the rats into six groups by giving them scores between 0 and 5. The scoring chart (Motor score) is shown in Figure 1.

When disease onset in the rats was diagnosed by their scoring <708 on the inclined plane test (muscle weakness onset), the affected rats were tested for righting reflex. If they were unable to right themselves from either side, they were given a score of 0. If they could right themselves from only one side but not the other, they were given a score of 1.

Rats that could right themselves from both sides were examined for the ability to stand in the cage as follows: Rats were observed in the home cage for 1 min to see if they would stand spontaneously (Step 1). When they moved little in the home cage or showed no tendency to stand during Step 1, they were stimulated by being transferred to another cage (Step 2), and then by being returned to their home cage again (Step 3); the transfers were done to activate exploration motivation. During Step 3, the rats were further stimulated by lightly knocking the cage to intensify the motivation to explore. Each step was carried out for 1 min and the test was stopped when the rat stood once. Rats were judged as "unable to stand" if they did not stand, even after all three steps.

Rats that did not stand were subjected to the next test in the open field, where the extent to which they dragged their bodies when moving was assessed. Those who always dragged and could not lift some parts of their bodies except for scrotums and tails at any time were given a score of 2. If

they could lift their dragging parts off the ground for even a moment, they were given a score of 3. The phenotype of dragging the forelimbs was different from that of dragging the hindlimbs. As disease progressed, "forelimb-type" rats first began to touch the tips of their noses on the ground, and then began to drag their head and upper trunk as they moved backward with their hindlimbs. "Hindlimb-type" rats dragged their lower trunk and moved forward with their forelimbs.

Finally, rats that had no abnormality in the above-mentioned assessments were examined in detail to see whether they had any observable functional deficits such as paralysis of the limbs or symptoms of general muscle weakness (e.g., walking with a limp, sluggish movement) in the open field. This condition could be judged subjectively and was defined as subjective onset. Rats with any of these symptoms were given a score of 4; otherwise they were given a score of 5.

Because the scores were based on subjective judgment, they might vary depending on the examiner. To examine inter-rater variability, three transgenic rats of different clinical types were examined according to the method described above, recorded on video tape, and subsequently scored by five observers from different backgrounds (Table I). The scores classified by the five observers were statistically analyzed for inter-rater agreement using Cohen's j statistics (Table II). Kappa values can range from 0 (no agreement) to 1.00 (perfect agreement), and can be interpreted as poor (<0.00), slight (0.00–0.20), fair (0.21–0.40), moderate (0.41–0.60), substantial (0.61–0.80), and almost perfect (0.81–1.00) (Landis and Koch, 1977). The scores for the three transgenic rats were, on the whole, quite consistent among the five observers, suggesting that the Motor score can be used as an objective method for assessing disease progression.

TABLE I. Motor Score of Transgenic Rats Assessed by Five Different Observers

Transgenic rat	Observer	0	1	2	3	4	5	6	7	8
#1407 Eventual hindlimb type										
	A	5	4	4		2	2	1	0	
	B	4	4	4		2	2	1	0	
	C	4	4	4		2	2	1	0	
	D	4	4	4		2	2	1	0	
	E	4	4	4		2	2	1	0	
	Mean	4.2	4	4		2	2	1	0	
#1470 Pure hindlimb type										
	A	5		4	4	2	2	2	2	0
	B	5		4	3	3	2	2	2	0
	C	5		4	3	2	2	2	2	0
	D	4		4	4	2	2	2	2	0
	E	4		4	3	2	2	2	2	0
	Mean	4.6		4	3.4	2.2	2	2	2	0
#1449 Pure forelimb type										
	A	4	3	3	3		2	1	1	0
	B	4	3	3	3		2	1	1	0
	C	3	3	3	3		2	1	1	0
	D	3	3	3	3		2	1	1	0
	E	4	3	2	2		2	1	1	0
	Mean	3.6	3	2.8	2.8		2	1	1	0

TABLE II. The kappa Statistics for Inter-Rater Agreement of Motor Score

| | Transgenic rat (clinical type) | | |
Observers	#1407 Eventual hindlimb	#1470 Pure hindlimb	#1449 Pure forelimb
A vs B	0.82	0.69	1.00
A vs C	0.82	0.82	0.83
A vs D	0.82	0.81	0.83
A vs E	0.82	0.70	0.69
B vs C	1.00	0.83	0.83
B vs D	1.00	0.53	0.83
B vs E	1.00	0.66	0.69
C vs D	1.00	0.64	1.00
C vs E	1.00	0.82	0.54
D vs E	1.00	0.81	0.54

TABLE III. Clinical Types of hSOD1 (G93A) Transgenic Rats

Clinical type	Subtype	n	%
Forelimb	Pure	4	8.2
	Eventual	5	10.2
Hindlimb	Pure	19	38.7
	Eventual	17	34.7
General		4	8.2
Total		49	100

Real-Time RT-PCR and Western Blot Analysis

Tissue specimens were dissected from the cerebral cortices, cerebella, medullae, and spinal cords (cervical, thoracic, and lumbar spinal cords) of the deeply anesthetized rats, and divided into two portions for total RNA and total protein preparation. Total RNA was isolated and first strand cDNA was synthesized as described previously (Okada et al., 2004). The real time RT-PCR analysis was carried out using Mx3000P (Stratagene, La Jolla, CA) with SYBR Premix Ex Taq (Takara Bio, Inc., Otsu, Japan). The primers used for the analysis were human SOD1 (5'-TTGGGCAATGTGACT-GCTGAC-3', 5'-AGCTAGCAGGATAACAGATGA-3'), rat SOD1 (5'-ACTTCGAGCAGAAGGCAAGC-3', 5'-ACATTG-GCCACACCGTCCTTTC-3', and b-actin (5'-CGTGGGCCG-CCCTAGGCACCA-3', 5'-TTGGCCTTAGGGTTCAGAGG-GG-3'). The results are presented as ratios of mRNA expression normalized to an inner control gene, b-actin. Total protein was prepared in lysis buffer containing 10 mM Tris-HCl (pH 7.6), 50 mM NaCl, 30 mM sodium pyrophosphate, 50 mM sodium fluoride, 20 mM glycerophosphate, 1% Triton X-100, and a protease inhibitor mixture (Complete; Roche Applied Science, Mannheim, Germany). Western blot analysis was carried out by a method established previously. In brief, a 5 1 g protein sample of an extract was run on 12% SDS-PAGE, transferred to nitrocellulose, and probed with anti-human SOD1 (1:1,000, mouse IgG, Novocastra Laboratories, Ltd., Benton Lane, UK), and anti-a-tubulin (1:2,000, mouse IgG, Sigma-Aldrich, Inc., Saint Louis, MO). Signals were detected with HRP-conjugated secondary antibodies (Jackson ImmunoResearch Laboratories, Inc., West Grove, PA) using an ECL kit (Amersham Bioscience UK limited, Little Chalfont, UK). Quantitative analysis was carried out with a Scion Image (Scion Corporation, Frederick, MD).

The amounts of proteins loaded in each slot were normalized to those of a-tubulin.

Immunohistochemical Analysis

Rats were deeply anesthetized (ketamine 75 mg/kg, xylazine 10 mg/kg, i.p.) and transcardially perfused with 4% paraformaldehyde/PBS (0.1 M PBS, pH 7.4) for histological examination. Spinal cord tissues were dissected out and post-fixed overnight in the same solution. Each spinal cord was dissected into segments that included the C6, T5, and L3 levels, immersed in 15% sucrose/PBS followed by 30% sucrose/ PBS at 48C, and embedded in Tissue-Tek O.C.T. Compound (Sakura Finetechnical Co., Ltd., Tokyo, Japan). Embedded tissue was immediately frozen with liquid nitrogen and stored at −808C. Serial transverse sections of each spinal segment were cut on a cryostat at a thickness of 14 1 m. The sections were pre-treated with acetone for 5 min, rinsed with PBS three times and permeabilized with TBST (Tris-buffered saline with 1% Tween 20) for 15 min at room temperature. After being blocked in the TNB buffer (Perkin-Elmer Life Sciences, Inc., Boston, MA) for 1 hr at room temperature, the sections were incubated at 48C overnight with an anti-choline acetyltransferase (ChAT) polyclonal antibody (AB144P, Goat IgG, 1:50; Chemicon International, Inc., Temecula, CA). After being washed with PBS three times, the sections were incubated for 2 hr at room temperature with a biotinylated secondary antibody (Jackson ImmunoResearch Laboratories, Inc.). Finally, the labeling was developed using the avidin-biotin-peroxidase complex procedure (Vectastain ABC kits; Vector Laboratories, Inc., Burlingame, CA) with 3,3-diaminobenzidine (DAB; Wako Pure Chemical Industries, Ltd., Osaka, Japan) as the chro-
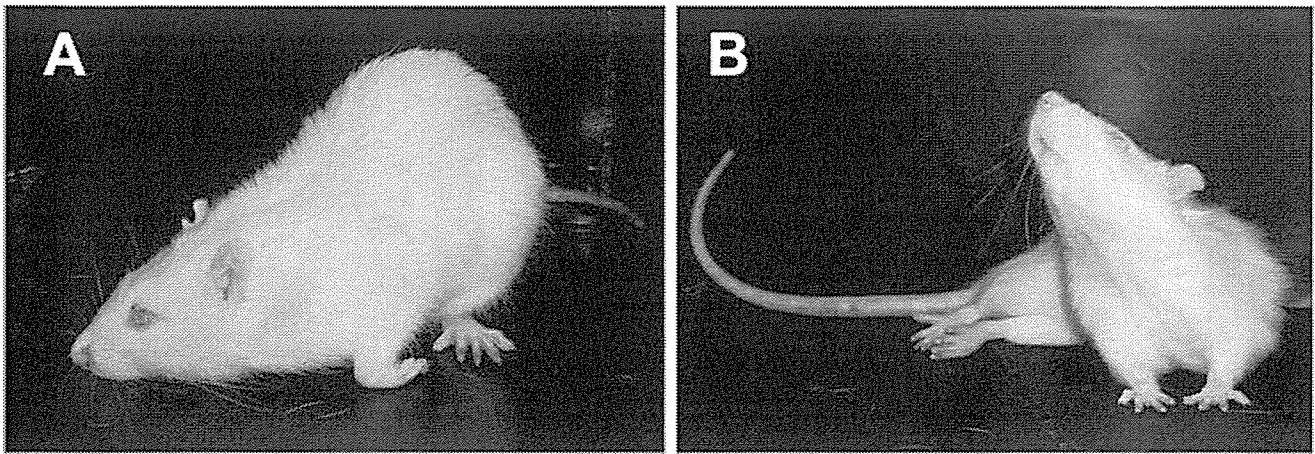
Fig. 2. Characteristic appearance of hSOD1 (G93A) transgenic rats. A: Forelimb type. The rat was unable to raise its head and was obligated to take a posture of raising the lumbar region, as indicated, because of the paralyzed forelimbs. B: Hindlimb type. The rat showed paraplegia, but was able to raise its head and upper trunk with its non-paralyzed forelimbs.

mogen. Immunohistochemical images were examined with a Zeiss-AxioCam microscope system.

Motor neurons bearing ChAT-immunoreactivity in laminae VII, VIII, and IX of the ventral horn were counted in every tenth section (5 sections total for each segment) for each of the C6, T5, and L3 segments. Only the neurons that showed labeling above background level and were larger than 20 1 m in diameter were counted. The numbers of motor neurons in all segments (C6, T5, and L3) were summed for each animal to evaluate not only the local motor neuron loss, but the generalized loss of motor neurons throughout the spinal cord of each animal (n = 3 for each genotype at each time point). We next examined the correlation between the number of residual motor neurons and the results of the functional analyses described in this study. Statistical analysis was carried out with two-tailed unpaired Student's t-test. A P-value of <0.05 was considered statistically significant.

RESULTS

Clinical Types of hSOD1 (G93A) Transgenic Rats

Because we noticed variations in the disease phenotypes expressed by the G93A rats, we classified 49 rats into three clinical categories according to the location of initial paralysis. The clinical types were: the forelimb type, hindlimb type, and general type (Table III). Rats whose paralysis started in the forelimbs and progressed to the hindlimbs were defined as the "forelimb type." In contrast, rats whose paralysis started from the hindlimbs and progressed to the forelimbs were defined as the "hindlimb type." A typical appearance for the forelimb and hindlimb types is shown in Figure 2. Other rats, which showed simultaneous paralysis in the forelimbs and hindlimbs, were categorized as the "general type".

In addition, we classified the forelimb- and hindlimb-type rats into two subtypes, the pure and eventual types, based on the timing of the initial paralysis (Table III). Rats of the pure type showed paralysis that was limited to one or more of the four limbs as the initial observable deficit. Those of the eventual type initially showed symptoms of general muscle weakness (e.g., walking with a limp, sluggish movement), but without unequivocal limb paralysis. In the eventual type animals, paralysis of one of the limbs became apparent later. The ratio of each subtype is shown in Table III.

Evaluation of Disease Progression in the hSOD1 (G93A) Transgenic Rats

Although the transgenic rats varied in their clinical types, all four measures of disease progression (body weight, inclined plane test, cage activity, and SCANET) showed significant differences between the transgenic and wild-type rats (Fig. 3).

In contrast to the continuous weight gain in wild-type rats, the body weight in the affected rats ceased to increase and gradually decreased, with peak body weight attained around 110–120 days of age (P < 0.05, after 112 days of age) (Fig. 3A).

In the inclined plane test, initially both the transgenic and wild-type rats uniformly scored 75–80 degrees, after several training trials. However, the transgenic rats showed a significant decline in performance compared to their wild-type littermates from 120 days of age (Fig. 3B).

In the cage activity measurement, the movements of the wild-type rats remained stable, whereas those of the transgenic rats declined rapidly after 125 days of age (Fig. 3C).

In the SCANET test, even the wild-type rats showed decreased movements for all parameters (M1, M2, RG) in the late observation period, though they showed no abnormality in their motor functions. This might be because they had acclimated to the SCANET cage. The movement score of the transgenic rats was consistently worse than that of the wild-type rats after

A   Body weight

B   Inclined plane

C   Cage activity

D   SCANET Move1

E   SCANET Move2
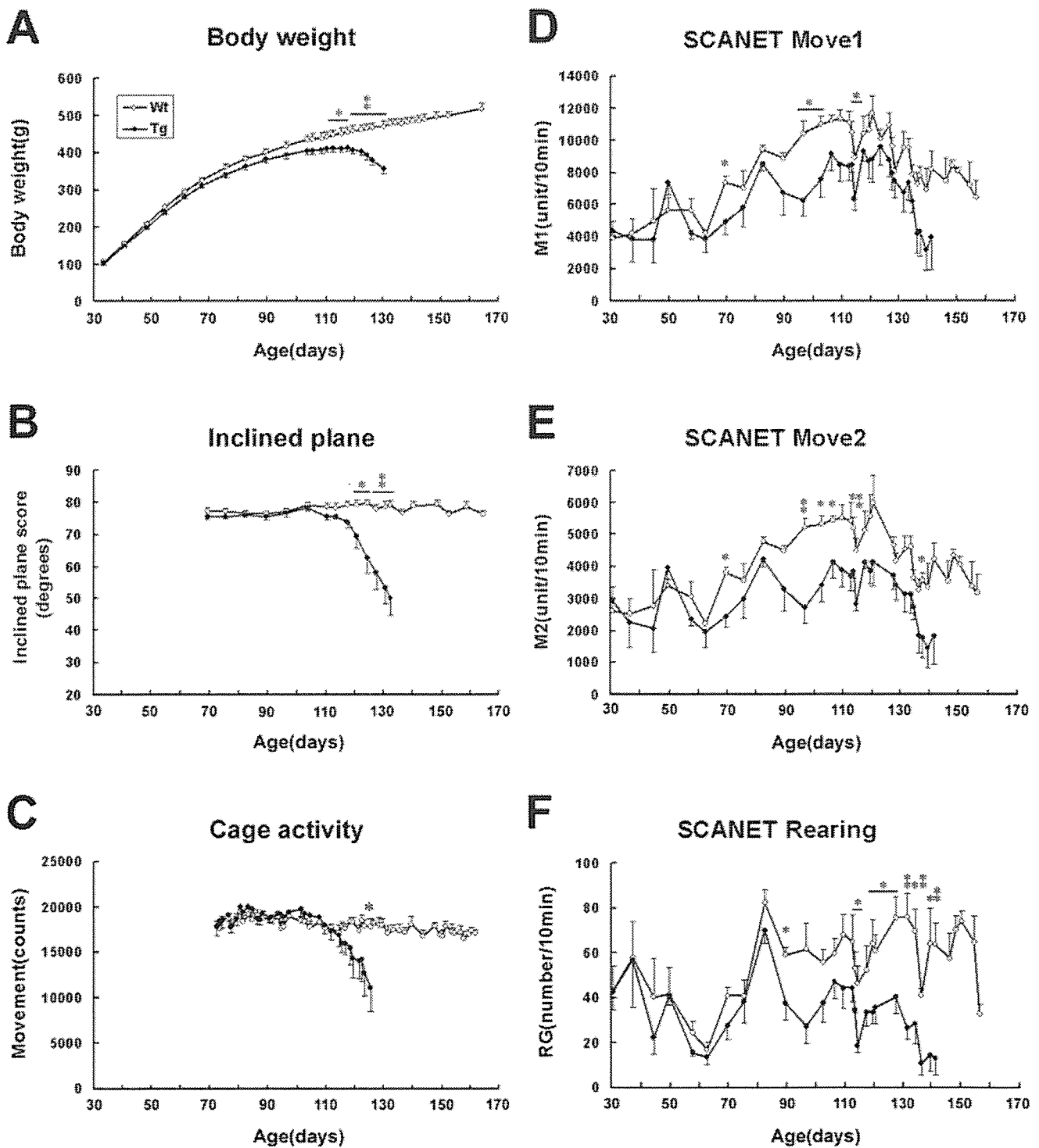

F   SCANET Rearing

Fig. 3. Disease progression in hSOD1 (G93A) transgenic rats monitored by four effective measures. A: Body weight. The weight gain of the transgenic group stopped at around 110–120 days. The difference became statistically significant at 112 days of age (n = 9 for each genotype). B: Inclined plane. The wild-type group scored 75–808 throughout the period, whereas the score of the transgenic group declined. The difference became statistically significant at 120 days of age (n = 9 for each genotype). C: Cage activity. The movements of the wild-type group were stable, whereas the scores of the transgenic group declined. Significance was reached at 125 days of age (n = 8

for each genotype). D–F: SCANET. For all parameters (M1, M2, RG), the movement scores of the transgenic group became constantly worse than those of the wild-type group after 60 days of age. The differences between the groups increased markedly after 90 days of age. Significance was attained beginning at 67 days of age for M1 and M2, and at 87 days of age for RG (n = 4 for each genotype). The comparison between the wild-type and transgenic groups was stopped when the first of the transgenic rats reached the end-stage of the disease and was sacrificed. Mean 6 SEM. *P < 0.05. **P < 0.01; two-tailed unpaired Student's t-test.

A   Body weight

B   Inclined plane
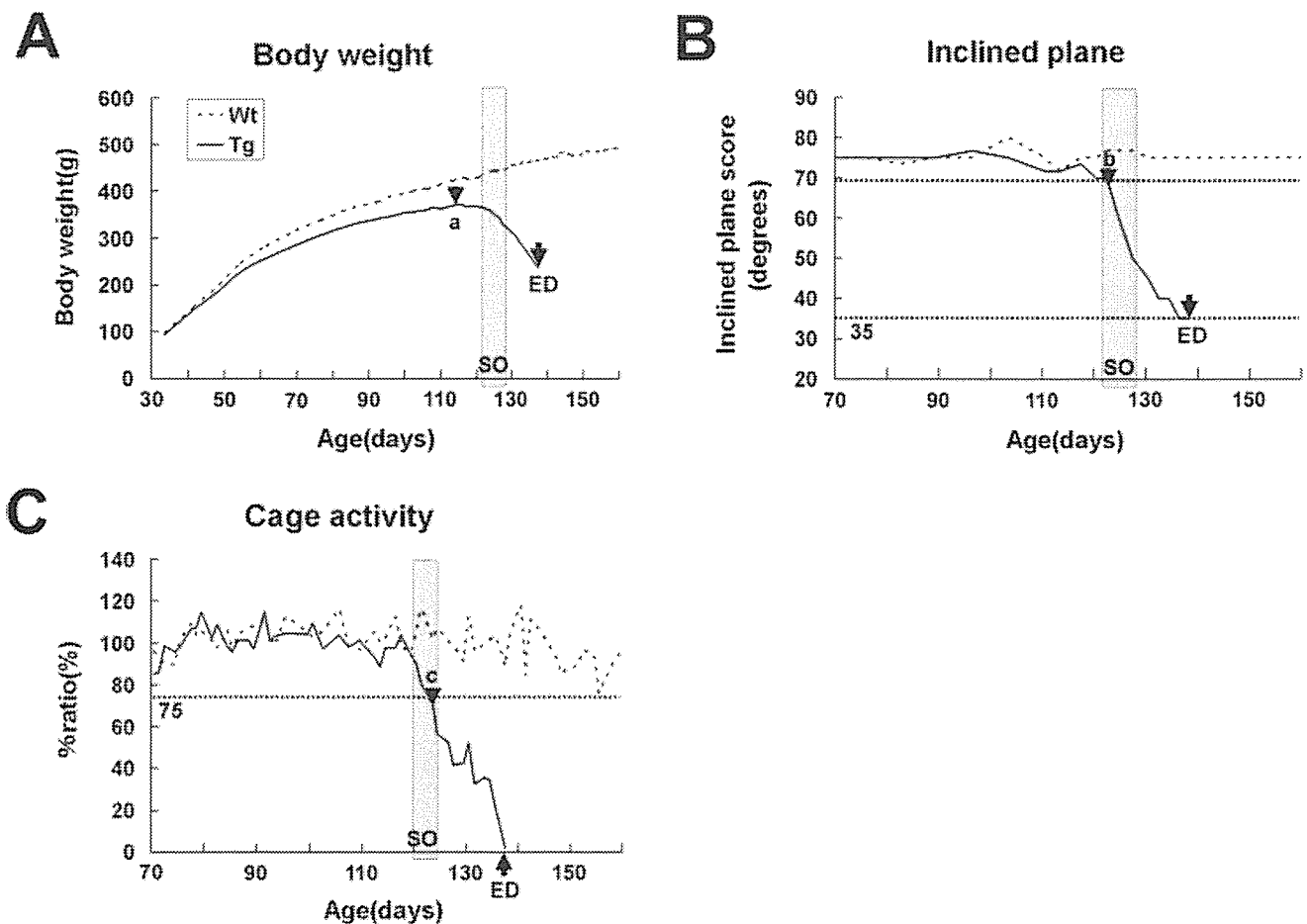

C   Cage activity

Fig. 4. Schematic presentation of the results from the body weight (A), inclined plane test (B), and cage activity (C) assessments. The onset defined by each measure (black arrowheads) and the end-stage of the disease (ED, black arrows) are indicated in the figures. a, pre-symptomatic onset: the day the transgenic rats scored their maximum body weight. b, muscle weakness onset: the earliest day the transgenic rats scored <70% in the inclined plane test. c, hypo-activity onset: the earliest day the transgenic rats scored <75% of the mean movements from 70–90 days of age in the cage activity measure. SO, subjective onset: the earliest day that observable functional deficits such as paralysis of the limbs or symptoms of general muscle weakness were observed subjectively in the open field (the gray shaded region in A–C).

60 days of age for all parameters (M1, M2, RG), how-ever, even after the wild-type animals showed the decrease in their movement scores. The differences between the two groups increased markedly after 90 days of age for M1, M2, and RG (Fig. 3D–F). The perform-ance of each rat fluctuated so markedly that the SCANET test seems to be inappropriate for statistical analysis.

Onset, End-Stage, and Duration of Disease in hSOD1 (G93A) Transgenic Rats

Using the quantitative analysis of disease progres-sion by body-weight measurement, the inclined plane test, and cage activity, as described above, we defined three time points of "objective onset," as shown in Figure 4. The SCANET results did not allow us to define a time of objective onset, because we could not establish a stable baseline level using the data from the

highly variable measurements we obtained, even for wild-type rats. The righting reflex failure was useful for detecting the time point of end-stage disease, which we defined as the generalized loss of motor activity in affected rats. A total of 20 transgenic rats assessed by body weight and the inclined plane test were analyzed for the day of objective onset, end-stage, and duration of the disease. The cage activity data from the eight transgenic rats were obtained simultaneously. The results are shown in Table IV.

The day the transgenic rats reached their maximum body weight was defined as pre-symptomatic onset (113.6 ± 4.8 days of age, black arrowhead in Fig. 4A, Table IV). This onset was judged retrospectively and always preceded the subjective onset (gray shaded region, Fig. 4A), which was determined by observable functional deficits in the open field, such as paralysis of limbs and symptoms of general muscle weakness. The

TABLE IV. Onset, End-Stage, and Duration in Days of Disease in hSOD1 (G93A) Transgenic Rats

Evaluation methods	Body weight and inclined plane (n = 20)	Cage activity (n = 8)
Objective onset		
Pre-symptomatic onset[a]	113.6 6 4.8 (103–124)	
Muscle weakness onset[b]	125.2 6 7.4 (110–144)	
Hypo-activity onset[c]		122.8 6 9.2 (109–139)[c]
Subjective onset (SO)[d]	126.5 6 7.1 (113–147)	121.3 6 9.8 (109–140)
End-stage disease (ED)[e]	137.8 6 7.1 (128–155)	134.1 6 8.2 (122–149)
Duration[f]		
ED-a[g]	24.3 6 6.5	
ED-b[h]	12.6 6 3.5	
ED-c[i]		11.4 6 1.3

Values are means 6 SD.
[a] Maximum of body weight.
[b] Less than 70 degrees in the inclined plane test.
[c] Less than 75% in the mean movements of 70-90 days in the cage activity.
[d] Observable functional deficits.
[e] Righting reflex failure.
[f] Difference in days between ED and each onset:
  [g] between ED and pre-symptomatic onset,
  [h] between ED and muscle weakness onset,
  [i] between ED and hypo-activity onset.

TABLE V. Comparison of the Onset, End-stage, and Duration in Days of Disease in the Forelimb-type and the Hindlimb-type Rats

	Forelimb type (n = 4)	Hindlimb type (n = 14)	General type* (n = 2)
Pre-symptomatic onset[a]	112.5 6 6.7	114.6 6 4.3	(108.5)
Muscle weakness onset[b]	125.8 6 2.8	126.7 6 7.3	(113.5)
End-stage disease (ED)[c]	134.0 6 2.4	140.1 6 7.1	(129.5)
Duration[d]			
ED-a[e]	21.5 6 8.5	25.5 6 6.2	(21)
ED-b[f]	8.3 6 1.0	13.4 6 3.0	(16)

Values are mean 6 SD.
* Values of general-type rats are listed in parenthesis for reference.
[a] Maximum of body weight.
[b] Less than 70 degrees in the inclined plane test.
[c] Righting reflex failure.
[d] Difference in days between ED and each onset:
  [e] between ED and pre-symptomatic onset,
  [f] between ED and muscle weakness onset.

pre-symptomatic onset was the most sensitive of all the onset measures described in this study (Table IV).

The first day the transgenic rats scored <708 in the inclined plane test was defined as the muscle weakness onset (black arrowhead, Fig. 4B). We could judge this onset prospectively. Muscle weakness onset (125.2 6 7.4 days of age, Table IV) was usually recorded before or at almost the same time as the subjective onset (8 days before to 1 day after, gray shaded region, Fig. 4B and 126.5 6 7.1 days of age, Table IV). The day the transgenic rats scored 358 or less on the inclined plane test coincided with the day of righting reflex failure (black arrow, Fig. 4B).

The first day the transgenic rats scored <75% of their baseline movements in the cage activity test was defined as hypo-activity onset (black arrowhead, Fig. 4C and 122.8 6 9.2 days of age, Table IV). We could also judge this onset prospectively. Hypo-activity onset was

recorded 1 day before to 4 days after the subjective onset (SO, shown as the gray shaded region in Fig. 4C and 121.3 6 9.8 days of age, Table IV). A 0% movement score for cage activity was seen at almost the same time as righting reflex failure (black arrow, Fig. 4C). Although disease onset and end-stage could be objectively defined with these methods, they had a wide range, of about 1 month, because of the diversity of the phenotypes (Table IV).

Differences in Disease Courses Between the Forelimb- and Hindlimb-Type Rats

Because we noticed variability in disease courses among different clinical types of hSOD1 (G93A) rats, we next assessed disease progression in 20 transgenic rats with forelimb- (n = 4), hindlimb- (n = 14), and general- (n = 2) type, using the probability of objective
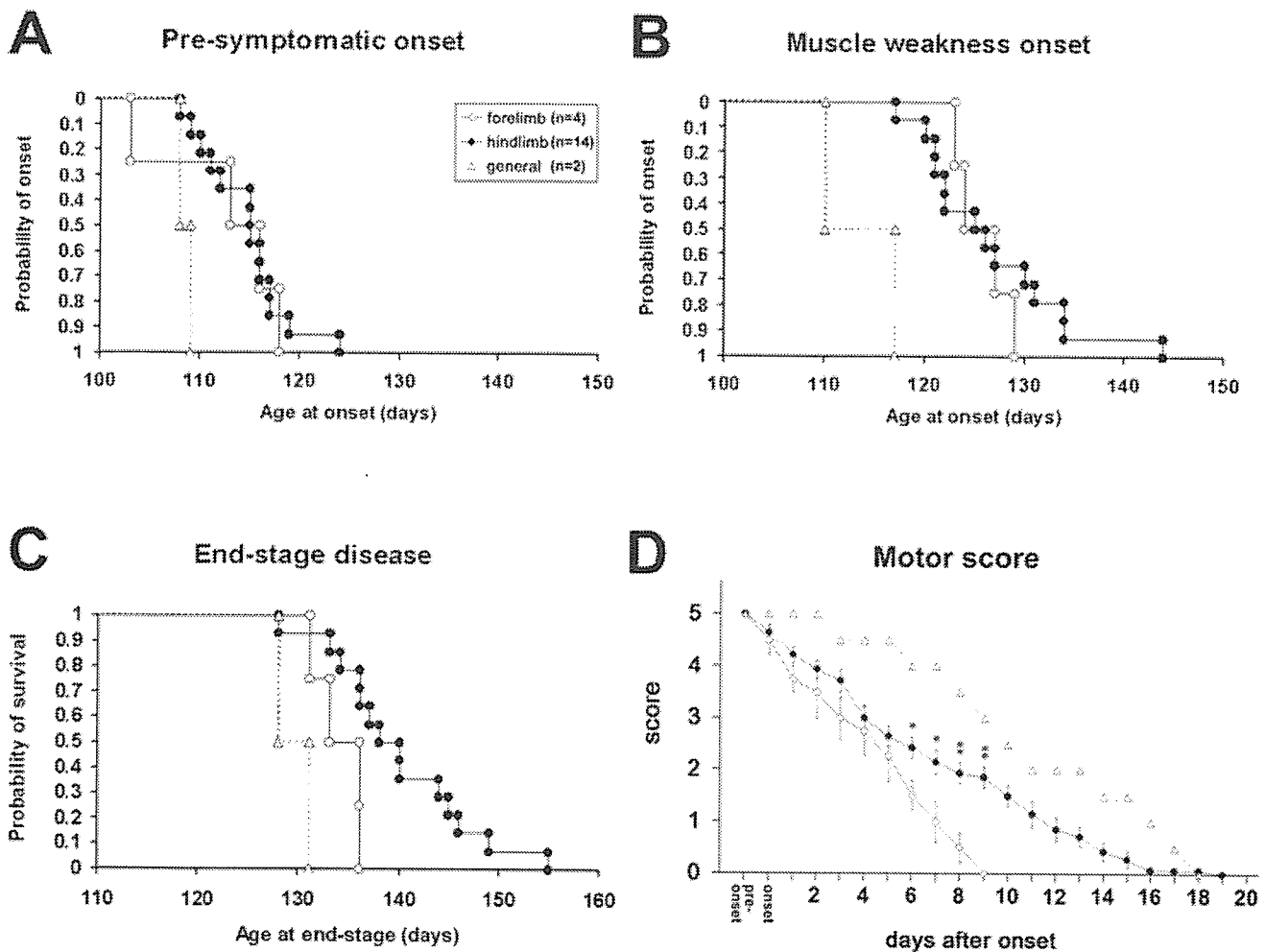
A Pre-symptomatic onset

B Muscle weakness onset

C End-stage disease

D Motor score

Fig. 5. Comparison of onset, end-stage, and disease progression in the forelimb-type (n = 4), and the hindlimb-type (n = 14) rats. Data from the general-type rats are also shown as dotted lines. A,B: The probability of the objective onsets. We did not see any differences in the probability of the objective onsets defined by body weight measurement (pre-symptomatic onset) and the inclined plane test (muscle weakness onset) between the forelimb- and hindlimb-type rats. C: The probability of survival as defined by end-stage disease. Survival was significantly shorter in the forelimb-type than in the hind-

limb-type rats (P < 0.05, Log-rank test). D: Assessment of disease progression using the Motor score. Affected rats were evaluated after muscle weakness onset. The forelimb type worsened more quickly than the hindlimb type. Score decline correlated well with the exacerbation of symptoms in both clinical types, clearly and objectively. Bars = means 6 SEM. Statistically significant differences between forelimb and hindlimb types are indicated in the figures. *P < 0.05. **P < 0.01; two-tailed unpaired Student's t-test.

onsets (pre-symptomatic onset and muscle weakness onset), the probability of survival defined by end-stage disease (failure in righting reflex), and the Motor score (Table V, Fig. 5). We did not see any differences in the objective onsets between the forelimb- and hindlimb-type rats (Fig. 5AB, Table V). However, survival as defined by end-stage disease was significantly shorter in the forelimb-type than in the hindlimb-type rats (P < 0.05, Log-rank test, Fig. 5C). Moreover, the duration of the disease calculated from the muscle weakness onset was also significantly shorter in the forelimb-type (8.3 6 1.0 days) than in the hindlimb-type rats (13.4 6 3.0 days) (see ED − b, P < 0.01, two-tailed unpaired Student's t-test, Table V).

The courses of functional deterioration evaluated by the Motor score after onset (muscle weakness onset) for each clinical type were well represented by the declines in their scores (Fig. 5D). The assessment by the Motor score also showed that disease progression in the forelimb type was more rapid than that in the hindlimb type (Fig. 5D).

Our results raise the question of why this variability in the disease course of each clinical type was observed. We speculated that there might be correlation between clinical type in G93A rats and the amount of locally expressed mutant hSOD1 (G93A) gene product. Therefore, we next investigated expression of the mutant hSOD1 gene in each segment of the spinal cord (cervical, thoracic, and lumbar) in the forelimb- and
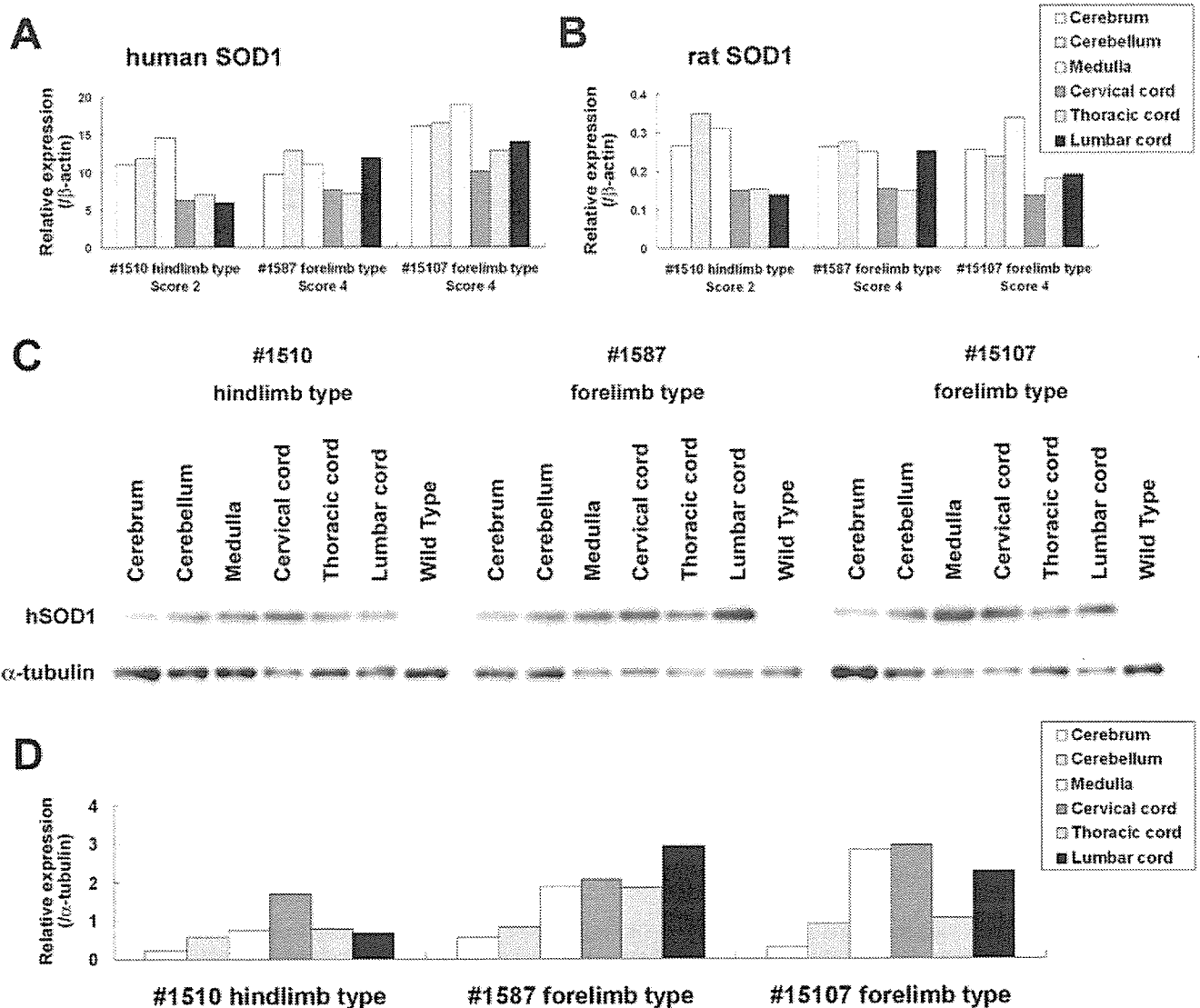
Fig. 6. The expression of mutant hSOD1 mRNA and protein in the cerebral cortex, cerebellum, medulla, and spinal cord (cervical, thoracic, and lumbar) of forelimb- and hindlimb-type rats. A,B: The amounts of human (A) and endogenous rat (B) SOD1 mRNA normalized to those of b-actin were quantified by real time RT-PCR analysis. C,D: Western blot analysis of the mutant hSOD1 protein was carried out in the same rats. Quantitative analysis was carried out with a Scion Image. The amounts of proteins were normalized to those of a-tubulin (D).

hindlimb-type rats by real time RT-PCR and Western blot analysis. However, at least at the stages after the apparent onset of muscle weakness, neither forelimb-type (#1587, Score 4 and #15107, Score 4) nor hind-limb-type rats (#1510, Score 2) necessarily expressed larger amounts of the mutant hSOD1 (G93A) transgene in the cervical cord or in the lumbar cord, respectively, at the mRNA and the protein level (Fig. 6). We also investigated the expression of endogenous rat SOD1 mRNA in the same rats by REAL TIME RT-PCR (Fig. 6B). Distribution of endogenous rat SOD1 mRNA expressed in each segment of the spinal cord showed almost the same pattern as that of mutant

hSOD1 mRNA. The expression of endogenous rat SOD1 mRNA was lower than that of mutant hSOD1 mRNA. Thus, we could not detect any definite correlation between the hSOD1 (G93A) transgene local expression profile in the spinal cord and the phenotypes of G93A rats for either the forelimb-type or the hind-limb-type rats (Fig. 6).

Reduction in the Number of Spinal Cord Motor Neurons at Different Disease Stages

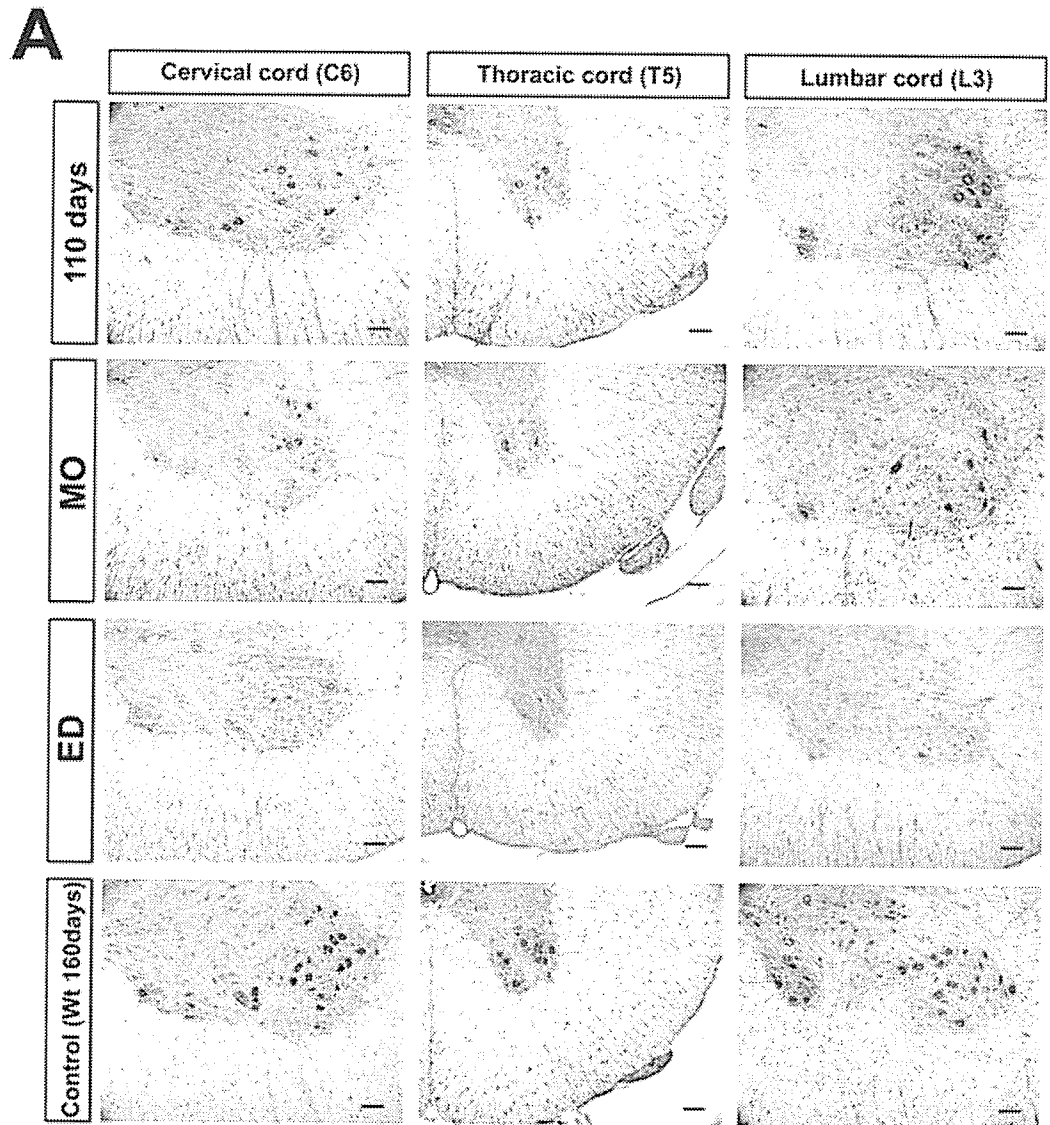We examined histo-pathological changes in the spinal cords of the transgenic rats in comparison with those

Fig. 7. The loss of motor neurons in the spinal cord of hSOD1 (G93A) transgenic rats at different stages. A: Immunohistochemical analysis of the spinal cord of transgenic rats. Transverse sections of the cervical (C6), thoracic (T5), and lumbar (L3) spinal cord of the transgenic rats and their wild-type littermates were stained with an anti-ChAT antibody to label viable motor neurons at the indicated stages (Scale bars = 100 l m). B: The number of ChAT immunoreactive motor neurons was counted and is shown in the histograms as the total number of motor neurons in the C6, T5, and L3 segments. This number began to decrease in the transgenic rats at 90 days of age, rapidly declined after 110 days of age, and fell to about 50% and 25% of wild-type rats at the muscle weakness onset (MO, around 125 days) and at end-stage disease (ED, around 140 days), respectively. Bars = means 6 SEM (n = 3 for each genotype). *P < 0.05. **P < 0.01; two-tailed unpaired Student's t-test.
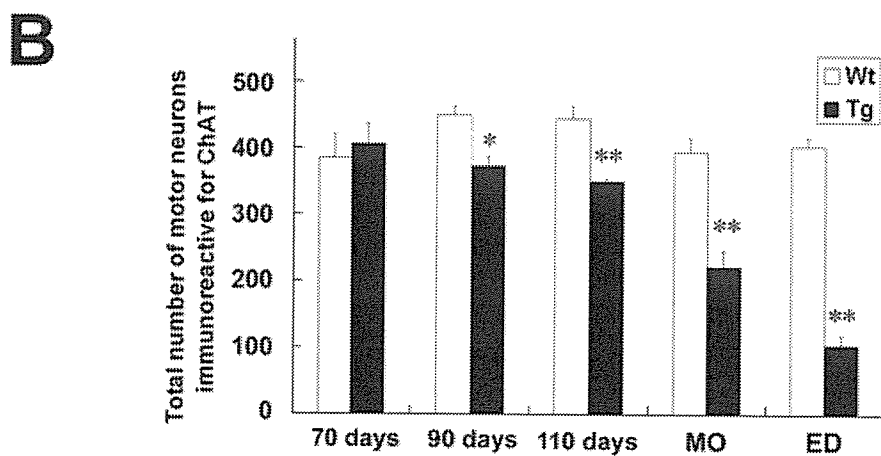
of their wild-type littermates at 70, 90, and 110 days of age, when the transgenic rats scored <708 in the inclined plane test (muscle weakness onset), and failed the righting reflex. To quantify the number of spinal motor neurons, we stained spinal cord sections of both groups with an anti-ChAT antibody.

As shown in Figure 7A, the numbers of ChAT immunoreactive motor neurons in the cervical (C6), thoracic (T5), and lumbar (L3) segments of the spinal cord decreased with disease progression. Quantitative analysis of the residual motor neurons showed that the total number of motor neurons in the transgenic rats began to decrease at 90 days of age, rapidly declined after 110 days of age, and fell to about 50% and 25% of the numbers in age-matched wild-type littermates at the time the score was <708 in the inclined plane test (muscle weakness onset) and of righting reflex failure, respectively (Fig. 7B).

DISCUSSION

Factors Underlying the Variability in Phenotypes of hSOD1 (G93A) Transgenic Rats

In previous studies of this G93A rat, only the hind-limb-type has been described, and the variety of phenotypes and variable clinical courses have not yet been mentioned (Nagai et al., 2001). Recently, however, another line of G93A rats backcrossed onto a Wistar background (SOD1$^{G93A/HWr}$ rats) was reported to present two phenotypes, including forelimb-type, and a large inter-litter variability in disease onset (Storkebaum et al., 2005). In the same way, commonly used FALS model mice harboring hSOD1 (G93A) gene have been reported to have clinical variability to some extent, and some of them dominantly show forelimb paralysis (Gurney et al., 1994). In this study, we recognized various clinical types, including forelimb-, hindlimb-, and general-type and established quantitative methods to evaluate disease progression that can be applied to any of the clinical types of this ALS model. We have also shown the variability in disease progression to depend on clinical types, that is, disease progression after the onset was faster in forelimb-type than in hindlimb-type rats. This difference may be due to the aggressiveness of the disease per se because we evaluated the time point of "death" (end-stage disease) according to righting reflex failure (Howland et al., 2002) to exclude the influence of feeding problems (bulbar region) and respiratory failure (level C2–C4).

These findings give rise to the next question; why is this variety of phenotypes and variability in the clinical course observed in the same transgenic line? There are at least three possible explanations. One is that the variation is due to the heterogeneous genetic background of the Sprague-Dawley (SD) rat (i.e., the strain used to generate this transgenic line), which might have led to different phenotypes. This idea is supported by the fact that the SD strain shows a large inter-individual disease variability in other models of neurodegenerative disorders, such as

TABLE VI. Adequacy of Evaluation Methods in Regard to Practical Use*

	Body weight	Inclined plane	Cage activity	SCANET	Motor score
Objectivity	A	B	A	A	B
Sensitivity	A	B	C	(A)	-
Specificity	C	B	C	C	A
Motivation independence	A	B	B	D	B
Skill requirements	A	B	A	A	B
Cost of apparatus	B	B	D	D	A

*A, more appropriate; B, appropriate; C, less appropriate; D, inappropriate.

Huntington's disease (Ouary et al., 2000). Similar phenotypic variability takes place in human FALS carrying the same mutations in hSOD1 gene (Abe et al., 1996; Watanabe et al., 1997; Kato et al., 2001), which could be explained by heterogeneous genetic backgrounds. Thus, the present transgenic ALS model rats may be highly useful to understand the mechanisms of bulbar onset, arm onset, or leg onset that are seen in human disease. There may be modifier genes of these phenotypes, which should be identified in the future study.

The second is that there is variability in the expression of the mutant hSOD1 protein. The transcriptional regulation of this exogenous gene could be affected by one or more unknown factors, such as epigenetic regulation, and may not be expressed uniformly throughout the spinal cord of each animal. Therefore, some rats might express mutant proteins more in the cervical spinal cord and others might express more in the lumber cord, possibly resulting in the forelimb type and hindlimb type, respectively. However, we found no definite correlation between local expression levels of the mutant hSOD1 mRNA/protein in the spinal cord and the phenotypes of these animals, using real time RT-PCR and western blot analysis after the onset of muscle weakness, when the clinical type of the transgenic rats could be defined (Fig. 6). Moreover, the pathological analysis showed no correlation between the number of residual motor neurons in each segment and the phenotypes of end-stage animals. However, because >50% of spinal motor neurons have already degenerated at the stage of muscle weakness onset, whether local expression of the mutant hSOD1 gene and segmental loss of motor neurons correlate with the clinical types of G93A rats should be further investigated by analyzing younger animals at a stage when motor neuron loss has not progressed as much.

The third explanation involves a structural property of the mutant hSOD1 (G93A) protein itself. It is now thought that mutations in the hSOD1 gene may alter the 3-D conformation of the enzyme and, in turn, result in the SOD1 protein acquiring toxic properties that cause ALS (Deng et al., 1993; Hand and Rouleau 2002). For instance, the hSOD1 (G93A) mutant protein has been reported to be susceptible to nonnative protein–protein interactions because of its mutation site and unfolded structure (Shipp et al., 2003; Furukawa and

Age (days)

| 80 | 95 | 110 | 125 | 140 | 155 |

Initiation of motor neuron loss
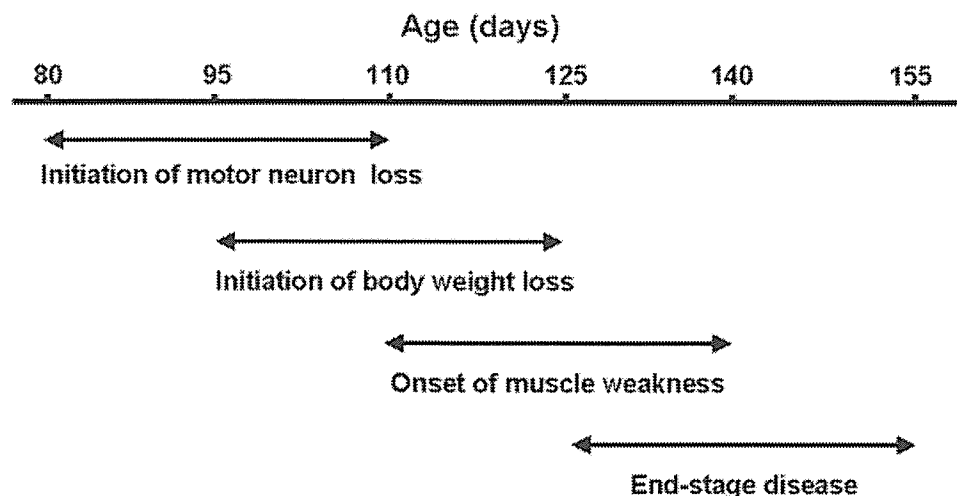
Initiation of body weight loss

Fig. 8. Four stages of disease progression in hSOD1 (G93A) transgenic rats. The disease progression can be classified into four stages as shown. The range for each stage is about 1 month and overlaps approximately 2 weeks with the next stage.

Onset of muscle weakness

End-stage disease

O'Halloran, 2005), suggesting that the G93A mutation might accelerate the formation of SOD1 protein aggregates, which may ultimately sequester heat-shock proteins and molecular chaperones, disturb axonal transport or protein degradation machineries, including the ubiquitin-proteasome system (Borchelt et al., 1998; Bruening et al., 1999; Williamson and Cleveland 1999; Okado-Matsumoto and Fridovich 2002; Urushitani et al., 2002). Curiously, the mutated hSOD1 (G93A) protein is more susceptible to degradation by the ubiquitin-proteasome system and has a shorter half-life than other mutants (Fujiwara et al., 2005), suggesting that it may cause more unstable toxic aggregates in the spinal cord than other mutations. The degradation rate is also affected by environmental factors unique to each animal, such as the progressive decline of proteasome function with age (Keller et al., 2000), and these factors could contribute to the variability of the clinical course of G93A rats.

Taking all these findings into consideration, the mutated hSOD1 (G93A) protein may gain properties that are responsible for a variety of phenotypes and variability in the clinical course of the affected animals.

Characteristics of Different Methods for Assessing hSOD1 (G93A) Transgenic Rats

The ideal measure is not influenced by the judgment of the observer, sensitive to small abnormalities, specific to detect pathologic events that are related to pathogenesis of the ALS-like disease, not influenced by the motivational factors of rats, minimal in the requirements for skill in the observer, and inexpensive to carry out. We assessed each evaluation method by the categories in regard to practical use as shown in the Table 6.

The initiation of body weight loss seems to be an excellent marker to detect the onset and should be highly recommended. Muscle volume might have already started to decrease, even in the period of continuous weight gain, as reported for hSOD1 (G93A) transgenic mice (Brooks et al., 2004). As a result, it could detect an abnormality relatively earlier than subjective

onset. The inclined plane test is considered to be the least defective method of all. It could objectively and specifically detect the decline in the muscle strength of these ALS model rats as a muscle weakness onset almost at the same time of the subjective onset. The cage activity measurement and SCANET require very expensive apparatus, and are limited by the availability of funds and space for making the measurements. Although SCANET test was most sensitive among these measures, it seems inappropriate for the statistical analysis, and does not add any more information than that obtained through simple observation of the rats because the performances of the rats might be severely affected by the extent of their motivation to explore. Motor score can specifically assess disease progression of each clinical type and is valuable in keeping the experimental costs at a minimum.

Correlation Between the Loss of Spinal Motor Neurons and Disease Stages

This study clearly shows the variable clinical course of G93A rats. According to our behavioral and histological analyses, we can divide the disease course of this transgenic model into four stages, whose durations have a range of about 1 month, as shown in Figure 8. Furthermore, we have established the pathological validity of the performance deficits detected by each measure of disease progression. "Initiation of motor neuron loss" was defined as a statistically significant decrease in the number of spinal motor neurons, which was found at around 90 days of age, but not 70 days of age (Fig. 7B). This coincides with, and seems to be sensitively detected by the marked difference in SCANET scores that begins at around 90 days of age (Fig. 3D–F). The "initiation of body weight loss" was usually detected at around 110 days of age as the peak body weight (pre-symptomatic onset, 113.6 6 4.8 days of age, range = 103–124, Table IV). This stage coincides with the initiation of a rapid decline in the number of motor neurons at around 110 days of age (Fig. 7B). "Onset of muscle weakness" was detected at around 125 days of age, as assessed by the

inclined plane test (muscle weakness onset, 125.2 6 7.4 days of age, range = 110–144, Table IV). This coincides with the number of spinal motor neurons in the transgenic rats being reduced to about 50% of the number in wild-type rats (Fig. 7B). We presume that transgenic rats do not present obvious muscle weakness until the number of motor neurons has been reduced to approximately half the number found in the healthy state. "End-stage disease" as defined by righting reflex failure was recorded at around 140 days of age (137.8 6 7.1 days of age, range = 122–155, Table IV). At this stage, the affected rats had only about 25% of the spinal motor neurons of age- and gender-matched wild-type rats (Fig. 7B), and showed a generalized loss of motor activity. Thus, our findings allow us to estimate the extent of spinal motor neuron loss by evaluating the disease stage with the measures described in this study.

In summary, we have described the variable phenotypes of mutant hSOD1 (G93A) transgenic rats and established an evaluation system applicable to all clinical types of these rats. Disease stages defined by this evaluation system correlated well pathologically with the reduction of motor neurons. Our evaluation system of this animal model should be a valuable tool for future preclinical experiments aimed at developing novel treatments for ALS.

ACKNOWLEDGMENTS

REFERENCES

Abe K, Aoki M, Ikeda M, Watanabe M, Hirai S, Itoyama Y. 1996. Clinical characteristics of familial amyotrophic lateral sclerosis with Cu/Zn superoxide dismutase gene mutations. J Neurol Sci 136:108–116.

Azzouz M, Ralph GS, Storkebaum E, Walmsley LE, Mitrophanous KA, Kingsman SM, Carmeliet P, Mazarakis ND. 2004. VEGF delivery with retrogradely transported lentivector prolongs survival in a mouse ALS model. Nature 429:413–417.

Barneoud P, Lolivier J, Sanger DJ, Scatton B, Moser P. 1997. Quantitative motor assessment in FALS mice: a longitudinal study. Neuroreport 8:2861–2865.

Borchelt DR, Wong PC, Becher MW, Pardo CA, Lee MK, Xu ZS, Thinakaran G, Jenkins NA, Copeland NG, Sisodia SS, Cleveland DW, Price DL, Hoffman PN. 1998. Axonal transport of mutant superoxide dismutase 1 and focal axonal abnormalities in the proximal axons of transgenic mice. Neurobiol Dis 5:27–35.

Brooks KJ, Hill MD, Hockings PD, Reid DG. 2004. MRI detects early hindlimb muscle atrophy in Gly93Ala superoxide dismutase-1 (G93A

SOD1) transgenic mice, an animal model of familial amyotrophic lateral sclerosis. NMR Biomed 17:28–32.

Brown RH Jr. 1995. Amyotrophic lateral sclerosis: recent insights from genetics and transgenic mice. Cell 80:687–692.

Bruening W, Roy J, Giasson B, Figlewicz DA, Mushynski WE, Durham HD. 1999. Up-regulation of protein chaperones preserves viability of cells expressing toxic Cu/Zn-superoxide dismutase mutants associated with amyotrophic lateral sclerosis. J Neurochem 72:693–699.

Chiu AY, Zhai P, Dal Canto MC, Peters TM, Kwon YW, Prattis SM, Gurney ME. 1995. Age-dependent penetrance of disease in a transgenic mouse model of familial amyotrophic lateral sclerosis. Mol Cell Neurosci 6:349–362.

de Belleroche J, Orrell R, King A. 1995. Familial amyotrophic lateral sclerosis/motor neurone disease (FALS): a review of current developments. J Med Genet 32:841–847.

Deng HX, Hentati A, Tainer JA, Iqbal Z, Cayabyab A, Hung WY, Getzoff ED, Hu P, Herzfeldt B, Roos RP, Warner C, Deng G, Soriano E, Smyth C, Parge HE, Ahmed A, Roses AD, Hallewell RA, Pericak-Vance MA, Siddique T. 1993. Amyotrophic lateral sclerosis and structural defects in Cu, Zn superoxide dismutase. Science 261:1047–1051.

Fujiwara N, Miyamoto Y, Ogasahara K, Takahashi M, Ikegami T, Takamiya R, Suzuki K, Taniguchi N. 2005. Different immunoreactivity against monoclonal antibodies between wild-type and mutant copper/zinc superoxide dismutase linked to amyotrophic lateral sclerosis. J Biol Chem 280:5061–5070.

Furukawa Y, O'Halloran TV. 2005. Amyotrophic lateral sclerosis mutations have the greatest destabilizing effect on the Apo- and reduced form of SOD1, leading to unfolding and oxidative aggregation. J Biol Chem 280:17266–17274.

Gale K, Kerasidis H, Wrathall JR. 1985. Spinal cord contusion in the rat: behavioral analysis of functional neurologic impairment. Exp Neurol 88:123–134.

Garbuzova-Davis S, Willing AE, Milliken M, Saporta S, Zigova T, Cahill DW, Sanberg PR. 2002. Positive effect of transplantation of hNT neurons (NTera 2/D1 cell-line) in a model of familial amyotrophic lateral sclerosis. Exp Neurol 174:169–180.

Gurney ME, Pu H, Chiu AY, Dal Canto MC, Polchow CY, Alexander DD, Caliendo J, Hentati A, Kwon YW, Deng HX, Chen W, Zhai F, Sufit RL, Siddique T. 1994. Motor neuron degeneration in mice that express a human Cu,Zn superoxide dismutase mutation. Science 264:1772–1775.

Hand CK, Rouleau GA. 2002. Familial amyotrophic lateral sclerosis. Muscle Nerve 25:135–159.

Howland DS, Liu J, She Y, Goad B, Maragakis NJ, Kim B, Erickson J, Kulik J, DeVito L, Psaltis G, DeGennaro LJ, Cleveland DW, Rothstein JD. 2002. Focal loss of the glutamate transporter EAAT2 in a transgenic rat model of SOD1 mutant-mediated amyotrophic lateral sclerosis (ALS). Proc Natl Acad Sci USA 99:1604–1609.

Inoue H, Tsukita K, Iwasato T, Suzuki Y, Tomioka M, Tateno M, Nagao M, Kawata A, Saido TC, Miura M, Misawa H, Itohara S, Takahashi R. 2003. The crucial role of caspase-9 in the disease progression of a transgenic ALS mouse model. EMBO J 22:6665–6674.

Kaspar BK, Llado J, Sherkat N, Rothstein JD, Gage FH. 2003. Retrograde viral delivery of IGF-1 prolongs survival in a mouse ALS model. Science 301:839–842.

Kato M, Aoki M, Ohta M, Nagai M, Ishizaki F, Nakamura S, Itoyama Y. 2001. Marked reduction of the Cu/Zn superoxide dismutase polypeptide in a case of familial amyotrophic lateral sclerosis with the homozygous mutation. Neurosci Lett 312:165–168.

Keller JN, Huang FF, Zhu H, Yu J, Ho YS, Kindy TS. 2000. Oxidative stress-associated impairment of proteasome activity during ischemia-reperfusion injury. J Cereb Blood Flow Metab 20:1467–1473.

Landis JR, Koch GG. 1977. The measurement of observer agreement for categorical data. Biometrics 33:159–174.

Mikami Y, Toda M, Watanabe M, Nakamura M, Toyama Y, Kawakami Y. 2002. A simple and reliable behavioral analysis of locomotor function after spinal cord injury in mice. Technical note. J Neurosurg Spine 97:142–147.

Mulder DW, Kurland LT, Offord KP, Beard CM. 1986. Familial adult motor neuron disease: amyotrophic lateral sclerosis. Neurology 36:511–517.

Nagai M, Aoki M, Miyoshi I, Kato M, Pasinelli P, Kasai N, Brown RH, Jr., Itoyama Y. 2001. Rats expressing human cytosolic copper-zinc superoxide dismutase transgenes with amyotrophic lateral sclerosis associated mutations develop motor neuron disease. J Neurosci 21:9246–9254.

Ohki-Hamazaki H, Sakai Y, Kamata K, Ogura H, Okuyama S, Watase K, Yamada K, Wada K. 1999. Functional properties of two bombesin-like peptide receptors revealed by the analysis of mice lacking neuromedin B receptor. J Neurosci 19:948–954.

Okada Y, Shimazaki T, Sobue G, Okano H. 2004. Retinoic-acid-concentration-dependent acquisition of neural cell identity during in vitro differentiation of mouse embryonic stem cells. Dev Biol 275:124–142.

Okado-Matsumoto A, Fridovich I. 2002. Amyotrophic lateral sclerosis: a proposed mechanism. Proc Natl Acad Sci USA 99:9010–9014.

Ouary S, Bizat N, Altairac S, Menetrat H, Mittoux V, Conde F, Hantraye P, Brouillet E. 2000. Major strain differences in response to chronic systemic administration of the mitochondrial toxin 3-nitropropionic acid in rats: implications for neuroprotection studies. Neuroscience 97:521–530.

Rivlin AS, Tator CH. 1977. Objective clinical assessment of motor function after experimental spinal cord injury in the rat. J Neurosurg 47:577–581.

Rosen DR, Siddique T, Patterson D, Figlewicz DA, Sapp P, Hentati A, Donaldson D, Goto J, O'Regan JP, Deng HX, Rahmani Z, Krizus A, McKenna-Yasek D, Cayabyab A, Gaston SM, Berger R, Tanzi RE, Halperin JJ, Herzfeldt B, van den Bergh R, Hung WY, Bird T, Deng G, Mulder DW, Smyth C, Laing NG, Soriano E, Pericak-Vance MA, Haines J, Reuleau GA, Gusella JS, Horvitz HR, Brown RH Jr. 1993. Mutations in Cu/Zn superoxide dismutase gene are associated with familial amyotrophic lateral sclerosis. Nature 362:59–62.

Shipp EL, Cantini F, Bertini I, Valentine JS, Banci L. 2003. Dynamic properties of the G93A mutant of copper-zinc superoxide dismutase as detected by NMR spectroscopy: implications for the pathology of familial amyotrophic lateral sclerosis. Biochemistry 42:1890–1899.

Storkebaum E, Lambrechts D, Dewerchin M, Moreno-Murciano MP, Appelmans S, Oh H, Van Damme P, Rutten B, Man WY, De Mol M, Wyns S, Manka D, Vermeulen K, Van Den Bosch L, Mertens N, Schmitz C, Robberecht W, Conway EM, Collen D, Moons L, Carmeliet P. 2005. Treatment of motoneuron degeneration by intracerebroventricular delivery of VEGF in a rat model of ALS. Nat Neurosci 8:85–92.

Sun W, Funakoshi H, Nakamura T. 2002. Overexpression of HGF retards disease progression and prolongs life span in a transgenic mouse model of ALS. J Neurosci 22:6537–6548.

Urushitani M, Kurisu J, Tsukita K, Takahashi R. 2002. Proteasomal inhibition by misfolded mutant superoxide dismutase 1 induces selective motor neuron death in familial amyotrophic lateral sclerosis. J Neurochem 83:1030–1042.

Wang LJ, Lu YY, Muramatsu S, Ikeguchi K, Fujimoto K, Okada T, Mizukami H, Matsushita T, Hanazono Y, Kume A, Nagatsu T, Ozawa K, Nakano I. 2002. Neuroprotective effects of glial cell line-derived neurotrophic factor mediated by an adeno-associated virus vector in a transgenic animal model of amyotrophic lateral sclerosis. J Neurosci 22: 6920–6928.

Watanabe M, Aoki M, Abe K, Shoji M, Iizuka T, Ikeda Y, Hirai S, Kurokawa K, Kato T, Sasaki H, Itoyama Y. 1997. A novel missense point mutation (S134N) of the Cu/Zn superoxide dismutase gene in a patient with familial motor neuron disease. Hum Mutat 9:69–71.

Weydt P, Hong SY, Kliot M, Moller T. 2003. Assessing disease onset and progression in the SOD1 mouse model of ALS. Neuroreport 14: 1051–1054.

Williamson TL, Cleveland DW. 1999. Slowing of axonal transport is a very early event in the toxicity of ALS-linked SOD1 mutants to motor neurons. Nat Neurosci 2:50–56.

Underediting of GluR2 mRNA, a neuronal death inducing molecular change in sporadic ALS, does not occur in motor neurons in ALS1 or SBMA

Yukio Kawahara [a,1], Hui Sun [a], Kyoko Ito [a], Takuto Hideyama [a], Masashi Aoki [b], Gen Sobue [c], Shoji Tsuji [a], Shin Kwak [a,*]

[a] Department of Neurology, Graduate School of Medicine, The University of Tokyo,
7-3-1 Hongo, Bunkyo-ku, Tokyo 113-8655, Japan
[b] Department of Neurology, Tohoku University Graduate School of Medicine, Sendai, Japan
[c] Department of Neurology, Nagoya University Graduate School of Medicine, Nagoya, Japan

Abstract

Deficient RNA editing of the AMPA receptor subunit GluR2 at the Q/R site is a primary cause of neuronal death and recently has been reported to be a tightly linked etiological cause of motor neuron death in sporadic amyotrophic lateral sclerosis (ALS). We quantified the RNA editing efficiency of the GluR2 Q/R site in single motor neurons of rats transgenic for mutant human Cu/Zn-superoxide dismutase (SOD1) as well as patients with spinal and bulbar muscular atrophy (SBMA), and found that GluR2 mRNA was completely edited in all the motor neurons examined. It seems likely that the death cascade is different among the dying motor neurons in sporadic ALS, familial ALS with mutant SOD1 and SBMA.
2005 Elsevier Ireland Ltd and the Japan Neuroscience Society. All rights reserved.

Keywords: ALS; SOD1; Spinal and bulbar muscular atrophy; Motor neuron; RNA editing; GluR2; AMPA receptor; Neuronal death

1. Introduction

Amyotrophic lateral sclerosis (ALS) is a progressive neurodegenerative disease with selective loss of both upper and lower motor neurons, and familial cases are rare. The etiology of sporadic ALS remains elusive but recently deficient RNA editing of AMPA receptor subunit GluR2 at the Q/R site is reported in motor neurons in ALS that occurs in a disease-specific and motor neuron-selective manner (Kawahara et al., 2004; Kwak and Kawahara, 2005). Moreover, underediting of the GluR2 Q/R site greatly increases the Ca^{2+} permeability of AMPA receptors (Hume et al., 1991; Verdoorn et al., 1991; Burnashev et al., 1992), which may cause neuronal death due to increased Ca^{2+} influx through the receptor channel, hence mice with RNA editing deficiencies at the GluR2 Q/R site die young (Brusa et al., 1995) and mice transgenic for an artificial Ca^{2+}-

permeable GluR2 develop motor neuron disease 12 months after birth (Kuner et al., 2005). Such evidence lends strong support to the close relevance of deficient RNA editing of the GluR2 at the Q/R site to death of motor neurons in sporadic ALS. However, although we and other researchers have demonstrated that dying neurons in several neurodegenerative diseases exhibit edited GluR2 (Kwak and Kawahara, 2005), it has not yet been demonstrated whether the underediting of GluR2 occurs in dying motor neurons in motor neuron diseases other than ALS. Such investigation is of particular importance since it will help clarify whether the molecular mechanism of motor neurons death is common among various subtypes of motor neurons.

ALS associated with the SOD1 mutation (ALS1) is the most frequent familial ALS (Rosen et al., 1993), and mutated human SOD1 transgenic animals have been studied extensively as a disease model of ALS1, yet the etiology of neuronal death in the animals has not been elucidated. Another example of non-ALS motor neuron disease is spinal and bulbar muscular atrophy (SBMA), which predominantly affects lower motor neurons with a relatively slow clinical course. Since the CAG

---
* Corresponding author. Tel.: +81 3 5800 8672; fax: +81 3 5800 6548.
E-mail address: kwak-tky@umin.ac.jp (S. Kwak).
[1] Present address: The Wistar Institute, Philadelphia, PA, USA.

Table 1
RNA editing efficiency of single motor neurons in SBMA

Case	Age at death (year)	Sex	No. of CAG repeats[a]	Postmortem delay (h)	GluR2(+) MN[b]	MN with 100% editing efficiency (% of GluR2(+) MN)
SBMA, case 1	71	M	48	2.5	12	12 (100)
SBMA, case 2	78	M	42	2.5	16	16 (100)
SBMA, case 3	60	M	44	1	16	16 (100)

[a] Number of CAG repeats in the androgen receptor gene.
[b] Motor neurons in which GluR2 RT-PCR amplifying product was detected.

repeat expansion in the androgen receptor gene has been demonstrated in SBMA (La Spada et al., 1991), and pharmacological castration is therapeutically effective in animal models (Katsuno et al., 2002, 2003), the death cascade responsible for SBMA is likely different from sporadic ALS. In this paper, an investigation is carried out into whether or not the dying mechanism underlying sporadic ALS is the same as ALS1 and SBMA by determining the editing status of the GluR2 Q/R site in single motor neurons.

2. Materials and methods

The animals used in this study were SOD1^{G93A} and SOD1^{H46R} transgenic male rats (Nagai et al., 2001) (n = 3 each) that had exhibited progressive neuromuscular weakness with their littermates as the control (n = 3 each) (Table 2). The first sign of disease in these rats was weakness of their hindlimbs, mostly exhibited by the dragging of one limb. Onset of motor neuron disease was scored as the first observation of abnormal gait or evidence of limb weakness. The mean age of onset of clinical weakness for the SOD1^{G93A} and SOD1^{H46R} lines was 122.9 ± 14.1 and 144.7 ± 6.4 days, respectively. As the disease progressed, the rats exhibited marked muscle wasting in their hindlimbs, and then in the forelimbs. The mean duration after the clinical expression of the disease in the SOD1^{G93A} and SOD1^{H46R} lines was 8.3 ± 0.7 and 24.2 ± 2.9 days, respectively (Nagai et al., 2001). The rats were killed 3 days and 2 weeks after the onset for the SOD1^{G93A} and SOD1^{H46R} lines, respectively, and we examined their fifth lumbar cord. Animals were handled according to Institutional Animal Care and Use Committee approved protocols that are in line with the Guideline for Animal Care and Use by the National Institute of Health. Spinal cords were isolated after deep pentobarbiturate anesthesia. In addition, spinal cords were obtained at autopsy from three genetically confirmed patients with SBMA (Table 1). Written informed consent was obtained from all subjects prior to death or from their relatives, and the Ethics Committees of Graduate School of Medicine, the University of Nagoya and the University of Tokyo approved the experimental procedures used. Spinal cords were rapidly frozen on dry ice and maintained at −80 °C until use.

Table 2
RNA editing efficiency of single motor neurons in mutated human SOD1 transgenic rats

Case (n)	GluR2(+) MN[a]	MN with 100% editing efficiency (% of GluR2(+) MN)
SOD1^{G93A}-1	13	13 (100)
SOD1^{G93A}-2	21	21 (100)
SOD1^{G93A}-3	21	21 (100)
SOD1^{H46R}-1	19	19 (100)
SOD1^{H46R}-2	23	23 (100)
SOD1^{H46R}-3	20	20 (100)
SOD1^{G93A}, littermates (3)	22	22 (100)
SOD1^{H46R}, littermates (3)	20	20 (100)

[a] Motor neurons in which GluR2 RT-PCR amplifying product was detected.

Single motor neurons were isolated and collected into respective single test tubes that contained 200 ml of TRIZOL Reagent (Invitrogen Corp., Carlsbad, CA, USA) using a laser microdissection system as previously described (Kawahara et al., 2003b, 2004) (LMD, Leica Microsystems Ltd., Germany) (Fig. 1a). After extracting total RNA from single neuron tissue, we analyzed the RNA editing efficiency at the GluR2 Q/R site by means of RT-PCR coupled with digestion of the PCR amplified products with a restriction enzyme Bbv-1 (New England BioLabs, Beverly, MA, USA) (Takuma et al., 1999; Kawahara et al., 2003a, 2004), and the editing efficiency was calculated by quantitatively analyzing the digests with a 2100 Bioanalyser (Agilent Technologies, Palo Alto, CA, USA), as previously described (Kawahara et al., 2003a). Briefly, after gel purification using Zymoclean Gel DNA Recovery Kit according to the manufacturer's protocol (Zymo Research, Orange, CA, USA), PCR products were quantified using a 2100 Bioanalyser. An aliquot (0.5 mg) was then incubated at 37 °C for 12 h with 10 × restriction buffer and 2 U of BbvI in a total volume of 20 ml and inactivated at 65 °C for 30 min. The PCR products had one intrinsic BbvI recognition sites, whereas the products originating from unedited GluR2 mRNA had an additional recognition site. Thus, restriction digestion of the PCR products originating from edited rat (278 bp) and human (182 bp) GluR2 mRNA should produce two bands (human GluR2 in parenthesis) at 219 (116) and 59 (66) bp, whereas those originating from unedited GluR2 mRNA should produce three bands at 140 (81), 79 (35), and 59 (66) bp. As the 59 (66) bp band would originate from both edited and unedited mRNA, but the 219 (116) bp band would originate from only edited mRNA, we quantified the molarity of the 219 (116) and 59 (66) bp bands using the 2100 Bioanalyser and calculated the editing efficiency as the ratio of the former to the latter for each sample.

The following primers were used for PCR for rat and human GluR2 (amplified product lengths are also indicated): for rat GluR2 (278 bp): rF (5′-AGCAGATTTAGCCCCTACGAG-3′) and rR (5′-CAGCACTTTCGAT-GGGAGACAC-3′). for human GluR2, the first PCR (187 bp): hG2F1 (5′-TCTGGTTTTCCTTGGGTGCC-3′) and hG2R1 (5′-AGATCCTCAGCACT-TTCG-3′); for the nested PCR (182 bp): hG2F2 (5′-GGTTTTCCTTG-GGTGCCTTTAT-3′) and hG2R2 (5′-ATCCTCAGCACTTTCGATGG-3′). We confirmed that these primer pairs were situated in two distinct exons with an intron between them and did not amplify products originating from other GluR subunits (data not shown). PCR amplification for rat GluR2 was initiated with a denaturation step that was carried out at 95 °C for 2 min, followed by 40 cycles of 95 °C for 30 s, 62 °C for 30 s, and 72 °C for 1 min. PCR amplification for human GluR2 began with a 1 min denaturation step at 95 °C, followed by 35 cycles of denaturation at 95 °C for 10 s, annealing at 64 °C for 30 s and extension at 68 °C for 60 s. Nested PCR was conducted on 2 ml of the first PCR product under the same conditions with the exception of the annealing temperature (66 °C).

3. Results

The number of motor neurons was severely decreased in the spinal cord of SBMA patients, and we analyzed 44 neurons dissected from three cases (12 from case 1, 16 from cases 2 and 3). Restriction digestion of the PCR products yielded only 116 and 66 bp fragments but no 81 or 35 bp fragments as seen in ALS motor neurons in all the SBMA motor neurons examined. Likewise, restriction digestion of the PCR products from motor
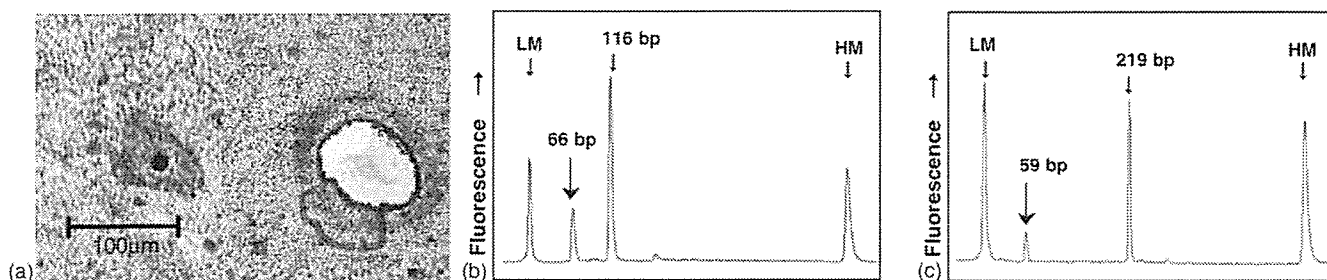
Fig. 1. (a) A single motor neuron from an SBMA patient before (left) and after (right) the dissection with a laser-microdissector. (b and c) An example of electropherogram by a 2100 Bioanalyser. Samples are the Bbv-1-digest of PCR product from tissues of a single motor neuron from an SBMA patient (b) and from a mutated human SOD1^{G93A} transgenic mouse (c). LM: lower marker (15 bp), HM: higher marker (600 bp).

neurons of mutated human SOD1 transgenic rats yielded only 219 and 59 bp fragments (Fig. 1). Therefore, the values of RNA editing efficiency at the Q/R site of GluR2 were 100% in 44 motor neurons from three SBMA cases (Table 1), 55 single motor neurons from three SOD1^{G93A} transgenic rats, 62 neurons from three SOD1^{H46R} transgenic rats, as well as in 42 neurons from three littermate rats of each group (Table 2). The consistent finding that the GluR2 Q/R site is 100% edited in motor neurons of SBMA patients and transgenic rats for mutated human SOD1 is in marked contrast to the finding in ALS motor neurons that the editing efficiency widely varied among neurons ranging from 0% to 100% (Kawahara et al., 2004).

4. Discussion

Compared to the significant underediting reported for the GluR2 Q/R site in motor neurons of sporadic ALS (Kawahara et al., 2004), GluR2 mRNA in all the examined motor neurons of the mutated human SOD1 transgenic rats with two different mutation sites and SBMA patients was completely edited at the Q/R site. We have confirmed that postmortem delay hardly influenced the editing efficiency at the GluR2 Q/R site (Kawahara et al., 2003b), hence the significant difference in the postmortem delay between the SBMA patients in this study and ALS patients in the previous report (Kawahara et al., 2004) would not have affected these results. We examined the motor neurons in the spinal cord segment corresponding to the hindlimb of mutated human SOD1 transgenic rats after their hindlimbs had become weak, indicating that the motor neurons examined were already pathologically affected. Likewise, we found that only a small number of motor neurons remained in the spinal cord of SBMA patients. Thus our results indicate that GluR2 RNA editing was complete in the dying motor neurons in both the mutated human SOD1 transgenic rats and SBMA patients, implying that the neuronal death mechanism is not due to the underediting of GluR2 mRNA seen in sporadic ALS. Since the pathogenic mechanism underlying ALS1 is considered to be the same as in mutant human SOD1 transgenic animals, motor neurons in affected ALS1 patients would be expected to have only edited GluR2 mRNA. Indeed, an association study of the SOD1 gene in a considerable number of patients with sporadic ALS reported no significant association with mutations of the SOD1 gene (Jackson et al., 1997). Due to

the lack of appropriate animal model for sporadic ALS, mutant human SOD1 transgenic animals have been used as a model for ALS in general, particularly in studies searching for therapeutically effective drugs. However, it should be kept in mind that mutated human SOD1 transgenic animals are merely a suggestive model for sporadic ALS and a gain of toxic function in mutated SOD1 kills motor neurons via mechanisms other than the demise of RNA editing. There are likely multiple different death pathways in motor neurons, and motor neurons in sporadic ALS, ALS1 and SBMA die by different death cascades.

Acknowledgements

References

Brusa, R., Zimmermann, F., Koh, D., Feldmeyer, D., Gass, P., Seeburg, P., Sprengel, R., 1995. Early-onset epilepsy and postnatal lethality associated with an editing-deficient GluR-B allele in mice. Science 270, 1677–1680.

Burnashev, N., Monyer, H., Seeburg, P., Sakmann, B., 1992. Divalent ion permeability of AMPA receptor channels is dominated by the edited form of a single subunit. Neuron 8, 189–198.

Hume, R.I., Dingledine, R., Heinemann, S.F., 1991. Identification of a site in glutamate receptor subunits that controls calcium permeability. Science 253, 1028–1031.

Jackson, M., Al-Chalabi, A., Enayat, Z.E., Chioza, B., Leigh, P.N., Morrison, K.E., 1997. Copper/zinc superoxide dismutase 1 and sporadic amyotrophic lateral sclerosis: analysis of 155 cases and identification of a novel insertion mutation. Ann. Neurol. 42, 803–807.

Katsuno, M., Adachi, H., Doyu, M., Minamiyama, M., Sang, C., Kobayashi, Y., Inukai, A., Sobue, G., 2003. Leuprorelin rescues polyglutamine-dependent phenotypes in a transgenic mouse model of spinal and bulbar muscular atrophy. Nat. Med. 9, 768–773.

Katsuno, M., Adachi, H., Kume, A., Li, M., Nakagomi, Y., Niwa, H., Sang, C., Kobayashi, Y., Doyu, M., Sobue, G., 2002. Testosterone reduction prevents phenotypic expression in a transgenic mouse model of spinal and bulbar muscular atrophy. Neuron 35, 843–854.

Kawahara, Y., Ito, K., Sun, H., Aizawa, H., Kanazawa, I., Kwak, S., 2004. RNA editing and death of motor neurons. Nature 427, 801.

Kawahara, Y., Ito, K., Sun, H., Kanazawa, I., Kwak, S., 2003a. Low editing efficiency of GluR2 mRNA is associated with a low relative abundance of